Int. J. Heat Mass Transfer. Vol. 32, No. 2, pp. 351–359, 1989
Printed in Great Britain

0017–9310/89 $3.00 + 0.00

Destratification and other properties of a packed bed heat store

BARRIE W. JONES and MAHYAR GOLSHEKAN
Physics Department, The Open University, Walton Hall, Milton Keynes MK7 6AA, U.K.

(*Received* 1 *July* 1987 *and in final form* 30 *June* 1988)

Abstract—A packed bed consisting of river pebbles is specified in some detail. Experimental data are presented on: the thermal conductivity and heat capacity of the bed; the pressure drop across the bed; the volumetric heat transfer coefficient between the airflow and the pebbles; destratification and cooling of the bed. These data are mutually consistent and are in good agreement with previously published work, where such exists, and with our own numerical models of the bed.

1. INTRODUCTION

THE STORAGE of heat and its subsequent recovery is a feature of a variety of energy systems, including process heat recovery and solar thermal supply. A well-known means of providing storage and recovery is the packed bed, in which a bed of solid particles is heated by a hot fluid flow, the heat being recovered later by the flow of cool fluid [1]. This recovery is usually achieved with *reversed* flow. This is because when a bed is heated it becomes hotter at the inlet end than at the outlet end, and the heating phase often ceases well before the temperature of the bed is everywhere raised by the same amount, thus leaving the bed thermally stratified at the end of such a charging phase [1]. Thus, recovery with *reversed* flow yields a fluid stream at the temperature of the hotter parts of the bed—a desirable outcome. Moreover, if destratification is slow then even if there is a long time between charging and recovery there will be little destratification loss of temperature of the heat recovered. In many applications of packed beds there can indeed be long times between charging and recovery, and thus persistent stratification is desirable in such cases.

Whereas there is a large amount of published work on the charging of packed beds and the recovery of heat from them, there is relatively little on their destratification. Dang-vu and Martin [2] have investigated the destratification of a large, horizontal airflow bed consisting of rounded pebbles with diameters in the range 35–65 mm. The observed destratification after several days can only be accounted for by a three-dimensional numerical model in which there is natural convection between the bottom and top of the bed. By contrast, over similar periods, Sullivan *et al.* [3] found no evidence for natural convection in vertical airflow beds consisting of river gravel. This might be because their solid particles are smaller, 18.1 ± 2.1 mm in one case and 29 ± 5 mm in another.

Thus, one aim of this present work was the further investigation of destratification and cooling of packed beds, via the study of the specific case of a packed bed consisting of river pebbles and with air as the fluid. The main objectives associated with this initial aim were:

(i) to measure individually the thermal properties of the packed bed that determine its destratification rate, namely its thermal conductivity k and thermal capacity $c = \rho c_p$ (see Nomenclature);

(ii) to investigate, by experiment coupled to a numerical model, destratification and cooling of the packed bed, including important container effects, and thus demonstrate whether the properties measured in (i) can help us predict destratification and cooling.

A second aim was the further investigation of the charging of packed beds, via the study of the same specific case as above. The main objectives here were:

(iii) to evaluate, by means of experiment coupled to a numerical model, the volumetric heat transfer coefficient h_{fs} between the pebbles and the airflow;

(iv) to measure the pressure drop Δp across the bed.

2. EQUIPMENT AND PROCEDURE

2.1. *The pebbles and their packing*

In order to characterize the pebbles we selected a random sample and for each pebble in the sample we determined its mineralogy, shape, mass m_i, and maximum dimension $\hat{d}_i$. For the whole sample we obtained the mean pebble density ρ_s by dividing the mass of the sample by the solid volume, the latter being obtained by a water displacement method.

The equivalent spherical diameter d_i of each pebble in a sample can in principle be obtained directly from its volume v_i. However, v_i can only be measured accurately for the largest pebbles and so, to obtain d_i we have used

$$d_i = (6m_i/\pi\rho_s)^{1/3}. \quad (1)$$

NOMENCLATURE

a, b constants in Δp vs $\dot{m}$ [Pa s kg^{-1}, Pa s^2 kg^{-2}]
A cross-sectional area of bed [m^2]
Bi Biot number of bed particles [—]
c; c_c thermal capacity: bed; container [J m^{-3} K^{-1}]
c_p; c'_p; c_{pf} specific heat capacity: bed; water; fluid [J kg^{-1} K^{-1}]
d_i; $\hat{d}_i$; d_r; d_s for a pebble: equivalent spherical diameter; maximum dimension; representative diameter; mean equivalent spherical diameter [m, mm]
e standard error of d_s [m, mm]
h_{fs} volumetric heat transfer coefficient between fluid flow and the bed [W m^{-3} K^{-1}]
$\mathbf{i}_r$; $\mathbf{i}_z$ unit vectors: r-coordinate; z-coordinate [—]
k; k_c thermal conductivity: bed; container [W m^{-1} K^{-1}]
l length of bed (along flow) [m]
m; m'; m_i mass: pebbles; water; single pebble [kg]
$\dot{m}$ mass flow rate of fluid through bed [kg s^{-1}]
n number of pebbles in a sample [—]
Δp pressure drop across bed [Pa]
r radial coordinate [m]
s standard deviation of d_s [m, mm]
t time [s, min]
T; T_a; T_f; T_i; T'_i; T_m temperature: bed; ambient; fluid; initial pebbles; initial water; mixture [K, °C]
v_i volume of a pebble [m^3]
z; Δz axial coordinate; difference in z [m].

Greek symbols
α; α_c thermal diffusivity: bed; container [m^2 s^{-1}]
ε bed porosity [—]
μ viscosity of fluid [N s m^{-2}]
ρ; ρ_f; ρ_s density: bed; fluid; mean pebble [kg m^{-3}].

This is tantamount to using $v_i = m_i/\rho_s$ and will lead to significant error only if pebbles with different densities are distributed unequally among the different pebble sizes. We anticipate no significant error, particularly because the density range among the pebbles does not seem to be large. From the d_i we have obtained, in the usual way, the mean equivalent spherical diameter d_s, the standard deviation s, the coefficient of variation s/d_s and the standard error of the mean $e(=s/\sqrt{n})$. We have also obtained a representative diameter d_r, defined by

$$d_r = \frac{1.241}{\rho_s^{1/3}} \frac{\Sigma m_i}{\Sigma m_i^{2/3}}. \tag{2}$$

This is to enable comparison with a correlation equation for pressure drop Δp given by Hollands and Sullivan [4].

Bed porosities ε have been determined for the actual beds used, using

$$\varepsilon = 1 - \rho/\rho_s \tag{3}$$

where ρ is the mass of the bed divided by its volume, and where ρ_s is for the sample as discussed above.

2.2. *Measurement of k and c_p*

The thermal conductivity k of the packed bed has been obtained from measurements on a separate bed, filled with pebbles from the same batch. The porosities of the two beds are the same to ~1%. We have used a transient method to measure k, called the *probe method* [5], in which power is fed at a constant rate to a long straight probe running along the (vertical) axis of the bed. The value of k is obtained from the rate at which the probe temperature rises at long times. Details of our work have been published elsewhere [6].

The specific heat capacity c_p of the packed bed has been obtained from measurements on two samples of pebbles, using the venerable method of mixtures [7]. This is a fairly straightforward method, suitable when measurements have to be made on a comparatively large mass of a medium to typify it. The value of c_p is given in the ideal case by

$$c_p = \frac{m' c'_p (T'_i - T_m)}{m(T_m - T_i)} \tag{4}$$

where the prime denotes a reference substance (usually water) of known properties, where T_i and T'_i are the initial temperatures of the pebbles and water, m and m' their masses, and where T_m is the temperature of the mixture formed by adding the pebbles to the water.

In our case each pebble sample (about 1.4 kg) was held in closed copper tubes in an oven for several hours, to come to an accurately known, spatially uniform, steady temperature (about 80°C). A somewhat smaller mass of distilled water was held in a styrofoam dewar at an accurately known temperature about 15°C below ambient so that when the warm pebbles were added to the water T_m (equation (4)) rose close to ambient temperature, and thus the mixture could equilibrate almost free from heat losses. The pebbles were transferred rapidly from the copper tubes to a light mesh bag in the water which was then raised and lowered (keeping the pebbles below the water surface)

to facilitate mixing. The temperature of the mixture was accurately recorded. All temperatures were measured with individually calibrated, encapsulated thermocouples. A correction to c_p ($\sim 1\%$) has been made for heat lost by the pebbles to the dewar. From c_p and ρ we obtain $c = \rho c_p$ for the bed.

2.3. *The experimental packed bed*

The packed bed is outlined in Fig. 1. It is cylindrical in cross-section and has thicker insulating walls in proportion to its size than a practical device would have. This is in order to reduce heat losses in such a comparatively small bed so that destratification is not obscured. The polystyrene rubble beneath the bed provides further insulation without significantly impeding airflow.

Bed temperatures are measured at each of the five levels 0–4 in Fig. 1, using calibrated platinum resistance thermometers (PRTs). At each of these levels one PRT is located in a pebble at the bed centre, another in the air at the bed centre, three in the air equi-spaced around the bed periphery, and one just outside the styrofoam container to measure ambient temperature. The foam rubber disk at level 0 serves to improve the definition of the temperature at level 0, this being the inlet temperature.

The pressure drop across the bed is measured by a liquid manometer and by a capacitance transducer in parallel. One set of pressure tappings is located just above level 0, the other set between the support mesh and the styrofoam rubble (Fig. 1), with four equi-spaced circumferential tappings in each set. Pressure readings were made before the foam rubber disk was laid on top of the bed.

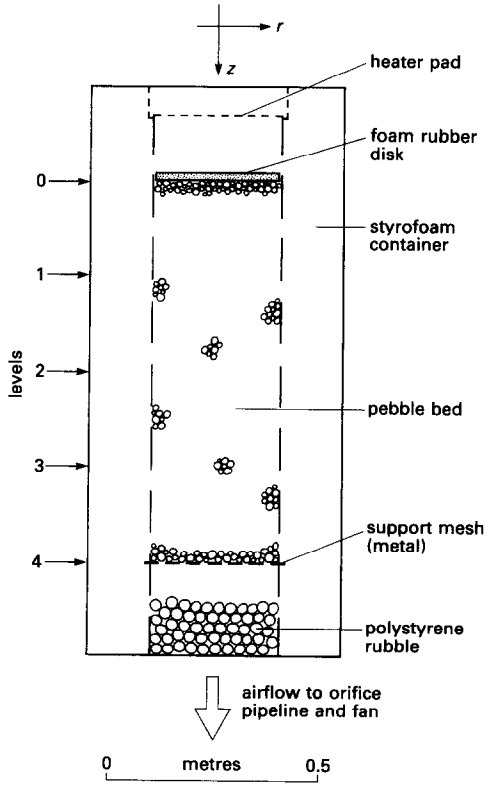

FIG. 1. The layout of the packed bed used to investigate Δp, h_{fs}, and destratification and cooling.

Airflow rate $\dot{m}$ is controlled by a gate valve, and is measured with an orifice pipeline set out in accord with the British Standard [8]. The pressure drop across the orifice plate is measured by a liquid manometer and by a capacitance transducer in parallel. Absolute pressure, temperature and humidity are measured so that the correct air density is used in obtaining $\dot{m}$. Heat is supplied to the bed by means of a heater pad located as shown in Fig. 1.

The pressure drop Δp across the bed was measured at various stages during the build-up of the bed. Then, with the foam rubber disk and the heater pad in place, a number of charging runs were performed, in each case after the bed had been allowed to come to a uniform temperature close to ambient. In some of these runs the bed was fully charged to facilitate determination of the volumetric heat transfer coefficient h_{fs}. In the other runs, the bed was only charged to about half its length, this being an optimum for studying destratification. In studying destratification the heater pad was removed after bed charging and the bed sealed to the top of the styrofoam container with a snug styrofoam plug.

2.4. *Analysis of experimental data*

We have analysed our experimental data with the aid of two numerical models, PKBED and HTCYL, that we have developed and implemented. These are both finite element models, time development being dealt with by the Adams–Bashforth–Moulton predictor–corrector method [9].

PKBED is a two-phase dynamic model, one-dimensional in z (Fig. 1). It was designed to describe the charging of (and recovery from) packed beds in which the fluid is a gas of negligible heat capacity. It is based on two equations [10] that can be written down for any section across the bed at any value of the axial coordinate z

$$\rho_f c_{pf} \varepsilon \left(\frac{\partial T_f}{\partial t}\right)_z = -\frac{\dot{m}}{A} c_{pf} \left(\frac{\partial T_f}{\partial z}\right)_t + h_{fs}(T - T_f) \quad (5)$$

$$\rho c_p (1-\varepsilon) \left(\frac{\partial T}{\partial t}\right)_z = h_{fs}(T_f - T) + h(T_a - T) + k \left(\frac{\partial^2 T}{\partial z^2}\right)_t. \quad (6)$$

In these equations the subscript f denotes the fluid, and the subscript a the ambient values. The unsubscripted quantities ρ, c_p and T are for the solid particles of the bed, and the quantities ε, A, h, k, z and t are for the bed as a whole. The symbol ρ denotes density, c_p the specific heat capacity, ε the bed porosity (void volume fraction), T the temperature, t the time, $\dot{m}$ the mass flow rate of fluid, A the cross-sectional area of the bed, h_{fs} the volumetric heat transfer coefficient, h

the heat transfer coefficient describing heat losses from the bed to the ambient surroundings, and k the thermal conductivity of the bed. The term in k represents destratification. *All* temperatures are functions of time, including the inlet fluid temperature, and all temperatures (except the fluid inlet temperature) are functions of position z. All other quantities are independent of time, position, and temperature.

When the fluid is air, $\rho_f c_{pf}$ is comparatively small, and so the left-hand side of equation (5) is set to zero. We then have the pair of equations that we have used, along with the following expression for h_{fs} [11]

$$h_{fs} = 650\left(\frac{\dot{m}}{A}\frac{1}{d_s}\right)^{0.7} \tag{7}$$

where d_s is the mean equivalent spherical diameter of the pebbles. In order to allow for the finite thermal diffusivity of individual pebbles we have incorporated a correction factor. This can be regarded as a multiplier of h_{fs} [12]. However, in our case this factor is very close to 1, in fact 0.99. The factor is given by $1/(1+Bi/5)$, where Bi is the Biot number of the pebbles.

Packed bed models for charging and recovery modes have been reviewed by Beasley and Clark [10]. Our model is of the more sophisticated kind among one-dimensional models in that it allows the inlet temperature of the fluid to vary with time, and in that it includes heat losses and destratification via the second and third terms respectively on the right-hand side of equation (6). However, heat losses have subsequently been treated differently (Section 3), and over the *charging* periods used in this work destratification is negligible. Therefore, *in effect* we are left with a fairly standard approach [10] to modelling the charging of (and recovery from) packed beds, and the main interest in our results lies in the accuracy with which equation (7) represents h_{fs}.

HTCYL is a one-phase dynamic model, two-dimensional in r and z (Fig. 1) and thus applies to axially symmetric cases. It was designed to describe the destratification of packed beds and the overall cooling that inevitably occurs during destratification. The simplification of one phase is fully justified provided that application of the model is delayed for a relatively short time after the end of charging to allow the two phases (fluid and solid) to come to the same temperature at any point in the bed.

HTCYL is based on the standard equation

$$\nabla\cdot(k\nabla T) = c\frac{\partial T}{\partial t} \tag{8}$$

where, in cylindrical polar coordinates, in the axially symmetric case

$$\nabla = \mathbf{i}_r\frac{\partial}{\partial r} + \mathbf{i}_z\frac{\partial}{\partial z} \tag{9}$$

where $\mathbf{i}_r$ and $\mathbf{i}_z$ are unit vectors in the radial and axial directions. In equation (8) k is thermal conductivity and c the thermal capacity ($=\rho c_p$). Both are functions of position. In our particular case we have k and c for the pebble bed, k_c and c_c for the cylindrical styrofoam container and for the styrofoam top plug, and other values for the polystyrene rubble and support mesh beneath the bed (Fig. 1).

Note that we *cannot* model the system by representing each region by thermal diffusivity α ($=k/c$) and then, in effect, joining these regions together. Such aggregation of k and c to form α fails to represent properly the behaviour at the interfaces, and this is crucial. In our particular case, at the bed/container interface, large c for the pebble bed meets small k_c for the styrofoam container. This generates a very large time constant c/k_c that largely controls the cooling rate of the bed.

More generally, for values of k, c, k_c, c_c of practical relevance (which includes our values), to a *first* approximation c/k_c is a measure of the overall cooling rate, and c/k is a measure of the destratification rate.

3. RESULTS

3.1. *The pebbles, pebble packing, k and c_p*

The pebbles came from the local Oxford clay. They were drawn from the standard commercial stock of a local quarry, and were washed and graded in accord with standard commercial practices. No further grading was performed by us, though we thoroughly washed the pebbles, and this removed most of the fine dust. The pebbles were allowed to dry before use.

Our stock consists of roughly equal quantities of flint and compact sandstone, with small quantities of quartzite and of other types. On a subjective basis roughly half can be described as angular, the remainder as rounded, the angular fraction being greater among the smaller pieces. Also, flints of all sizes tend to be angular. A random sample of our stock was selected, consisting of 163 pebbles, total mass 3.98 kg. Table 1 lists pertinent properties of this sample, as

Table 1. Properties of pebbles and of pebble samples

Property	Value	Comment
ρ_s	2530 ± 20 kg m^{-3}	from a random sample of 163 pebbles, at $\sim$20°C
d_s	24.3 mm	
d_r	28.7 mm	
s	7.1 mm	
s/d_s	0.29	
e	0.56 mm	
c_p	812 ± 10 J kg^{-1} K^{-1}	from two samples, 1.375 and 1.469 kg, average over $\sim$20 to $\sim$80°C
k	0.55 ± 0.01 W m^{-1} K^{-1}	for a 274.5 kg bed, $\rho = 1529\pm10$ kg m^{-3}, $\varepsilon = 0.396\pm0.01$, at $\sim$25°C
ρ	1525 ± 10 kg m^{-3}	for the 103.5 kg bed shown in Fig. 1
ε	0.397 ± 0.01	

outlined in Section 2.1. Table 1 also lists values of the specific heat capacity c_p of the pebbles and the thermal conductivity k of the bed, obtained as outlined in Section 2.2. The value of c_p has been obtained from two samples, masses 1.375 and 1.469 kg, and the value of k has been obtained from a second bed of mass 274.5 kg. The primary bed, laid out as in Fig. 1, and used for the charging, pressure drop and destratification studies central to this work, contains 103.5 kg of pebbles, and Table 1 gives the values of ρ and ε for this bed.

The values of c_p and k vary with temperature. The temperatures of our measurements are given in Table 1. To obtain values at other temperatures we have used a temperature coefficient of $\sim 0.001°C^{-1}$ for $(1/c_p)(dc_p/dT)$ and $\sim 0.002°C^{-1}$ for $(1/k)(dk/dT)$. The former value is a 'guesstimate' based on sparse data for various minerals in data handbooks, and the latter value is based on our experimental results. Neither coefficient is very accurate though in no case has a temperature adjustment exceeded 3%.

We have scrutinized our measurements of k for evidence of convective transport of heat in the packed bed. We conclude that there is negligible convective transport across the bed but that there might be significant convective transport within each pore, and, of course, particularly in the larger pores.

3.2. *Pressure drop* Δp

The pressure drop Δp across the bed in Fig. 1 was measured as the bed was built up. These measurements show that, as expected, Δp is proportional to bed length l (over the range 0.2–0.9 m) to within the $\pm 1\%$ uncertainty in the *relative* values of Δp.

When the bed was complete the airflow rate $\dot{m}$ was varied over the range 0.01–0.02 kg s^{-1}, and Δp then follows the relationship

$$\Delta p = a\dot{m} + b\dot{m}^2 \tag{10}$$

to within the $\pm 1\%$ uncertainties in the *relative* values of Δp and $\dot{m}$. This form of $\Delta p(\dot{m})$ is as expected [4].

The value of Δp we measured at the maximum flow rate of 0.0200 ± 0.0004 kg s^{-1} (gate valve fully open) is 70 ± 3 Pa at a bed temperature of $20 \pm 1°C$, where the uncertainties in $\dot{m}$ and Δp are in their absolute values. The correlation in ref. [4] for thoroughly washed particles (to eliminate dust) is

$$\Delta p = \frac{(1-\varepsilon)l}{\rho_f d_r}\left(\frac{\dot{m}}{A}\right)^2\left[26 + 800\frac{\mu}{d_r}\left(\frac{A}{\dot{m}}\right)\right] \tag{11}$$

where ε is bed porosity, ρ_f and μ are, respectively, the density and viscosity of the fluid, d_r the representative diameter given by equation (2), and A the cross-sectional area of the bed. For our bed this correlation gives 32 ± 4 Pa. At our maximum flow rate we lie outside the domain of this correlation in that the Reynolds number for our flow is then ~ 400, whereas equation (11) applies only up to ~ 150. However, at $\dot{m} = 0.0100 \pm 0.0004$ kg s^{-1}, which corresponds to a Reynolds number of ~ 200, we measured $\Delta p = 21 \pm 3$ Pa, whereas equation (11) gives 8.4 ± 1.3 Pa, and so we are left with a real discrepancy.

Another correlation in the domain of which we lie, but which is not explicitly for thoroughly washed particles, is given by Chandra and Willits [13]

$$\Delta p = \frac{\varepsilon^{-2.7} l}{\rho_f d_s}\left(\frac{\dot{m}}{A}\right)^2\left[1.7 + 185\frac{\mu}{d_s}\left(\frac{A}{\dot{m}}\right)\right] \tag{12}$$

where d_s is the mean equivalent spherical diameter of the pebbles. For our bed at maximum flow this correlation gives 59 ± 5 Pa. (The uncertainty here and in equation (11) arises mainly from the uncertainties in ε, $\dot{m}$ and d_s.) Our experimental value of Δp is thus only $\sim 16\%$ higher than that from equation (12)—not a serious discrepancy in correlations for Δp.

Hollands and Sullivan [4] point out that Δp can be greatly increased by dust in a packed bed and they believe that the differences between equation (11) and equations like equation (12) largely arise from the elimination of dust from their particles by thorough washing. However, our pebbles have also been thoroughly washed and so we are at variance with their conclusion. However, packed beds are so complex that perhaps such disagreement is not very surprising.

As the bed temperature varies, the centrifugal fan behaves in a manner such that Δp varies much less than $\dot{m}$. For an increase in bed temperature from 19 ± 1 to $33 \pm 1°C$ the measured value of Δp rose by $\lesssim 1\%$. The rise in Δp from equation (12), using new values of $\dot{m}$, ρ_f, and μ for this higher temperature, is 2 Pa to 61 ± 5 Pa. Thus, to within observational uncertainty there is no conflict between the observed variation of Δp with bed temperature, and that predicted by equation (12) (nor indeed with that predicted by equation (11)).

3.3. *Heat transfer coefficient* h_{fs}

Figure 2 shows the way in which the temperature profile in the bed in Fig. 1 built up during a typical charging period starting at $t = 0$. The airflow rate $\dot{m}$ and the temperature at level 0 serve to define the heat input rate to the bed. This rate is significantly less than the electrical power to the heater pad, mainly because the heater pad loses some energy by radiation upwards. The inlet temperature varied somewhat during charging, though at the two times into charging shown in Fig. 2 the level 0 temperatures happen to have been the same.

The temperatures in Fig. 2 are for air. We have not shown pebble temperatures, because the PRTs inside the pebbles influenced the pebble temperatures considerably. We noticed that the peripheral air temperatures at each level rose more rapidly during charging than the air temperature at the bed centre, until that level was nearly fully charged. Perhaps this is because the low thermal capacity and low thermal conductivity of the styrofoam container results in less cooling of the air near the bed periphery. We thus

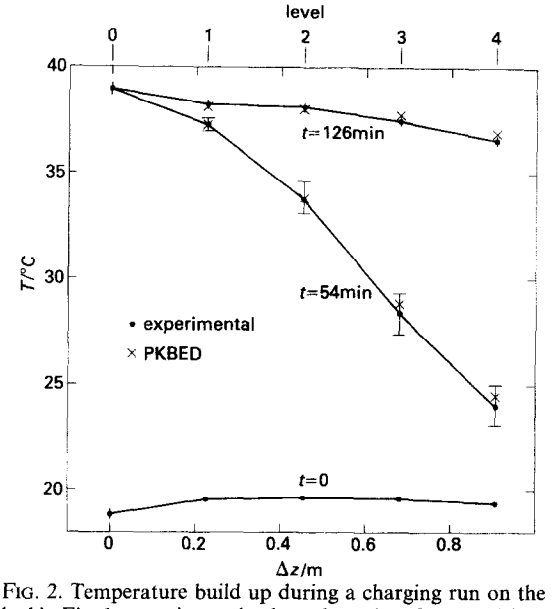

FIG. 2. Temperature build up during a charging run on the bed in Fig. 1: experimental values plus values from PKBED.

need to define an average temperature at each level, and here we are guided by the way the air temperatures relaxed during the early time parts of our destratification studies. This relaxation shows that the peripheral air temperature (from three PRTs) should be given equal weight to the temperature (from one PRT) at the bed centre. This weighting has been adopted in preparing Fig. 2. The difference between peripheral and central temperatures is greatest around half charge, and so the uncertainty in the average air temperature is greatest around this time, as shown in Fig. 2. Errors in Δz at levels 1–4 are the uncertainties in the locations of the PRTs with respect to level 0, and are shown only at $t = 54$ min for clarity.

In order to see whether small, undetected leaks could have significantly influenced the experimental values in Fig. 2 we deliberately introduced an obvious leak at level 0, larger than any undetected leaks. The effect on bed temperatures is sufficiently small that we are confident that the experimental values in Fig. 2 have *not* been significantly influenced by leaks.

The experimental data have been analysed with the aid of PKBED. Equation (6) shows that this numerical model includes heat losses via a simple heat conduction term through the container walls to ambient temperature. For the bed in Fig. 1 this is unlikely to be good enough, because the walls are so thick that the container during charging behaves more like a medium with thermal capacitance and conductance unconnected to ambient temperature. Therefore, we have instead used HTCYL to obtain an estimate of the wall temperature profile during charging and have hence deduced that to allow for heat losses to the container any bed temperature predicted by PKBED (with no heat losses) could be reduced by up to 5% of the difference between this predicted temperature and the temperature at $t = 0$, 4% being, overall, a best estimate. We have thus lowered the temperatures predicted by PKBED (with no heat losses) by 4% of this difference and the outcome is shown in Fig. 2. The values from PKBED depend on various parameters, such as bed porosity ε and mass flow rate $\dot{m}$, and so are subject to uncertainty, to $\sim \pm 0.5$°C at half charge, less at full charge.

We conclude that, to within the various uncertainties, there is satisfactory agreement between experiment and PKBED. One implication of this is that the simple correlation for h_{fs} in equation (7) is adequate for our purposes.

3.4. *Destratification and cooling*

To study destratification, charging was halted when the bed was about half charged—something like the state at $t = 54$ min in Fig. 2. Then the bed was sealed and a few hours allowed to elapse so that non-uniform temperatures across the bed cross-section due to non-uniform charging could die away. The subsequent experimental data for one run are shown in Fig. 3, $t = 0$ being when charging was halted and the bed sealed. (The level 1 temperatures are close to those at level 0, so they have been omitted for clarity.) The peripheral temperatures at each level are the average over the three peripheral PRTs, and the bed centre temperatures the average over the two central PRTs, though temperature differences within each group are much less than between the two groups, the periphery now being cooler than the centre (as expected). At level 4 there is little difference between the periphery and the centre, because of the metal support mesh (Fig. 1). This mesh has been modelled in HTCYL, as a local increase of the thermal conductivity of the bed in the r-direction.

In Fig. 3 a representative ambient temperature is also shown. Note that the bed temperatures respond to the ambient variations, with a time lag of several hours.

We estimate that the observational uncertainty in the bed temperatures in Fig. 3 is about ± 0.1°C.

Figure 3 also shows output data from HTCYL. The *input* data to HTCYL consist of the following measured values: bed and container dimensions; the thermal conductivity k and thermal capacity c of the pebble bed, obtained as outlined in Section 2.2, c being corrected to allow for the difference between the average temperature of measurement of c_p of ~ 50°C and the bed temperatures of ~ 30°C; values from the manufacturer of k_c and c_c for the styrofoam container; initial temperatures; ambient temperatures throughout destratification. The input values of k, c, k_c and c_c are given in the caption to Fig. 3.

For these input values the level of agreement in Fig. 3 between the HTCYL output and the experimental data is satisfactory. As expected, the HTCYL output is a good deal more sensitive to the values of k, c, and k_c than to the value of c_c. Overall, the sensitivity analysis bears out the statement in Section 2.4 that, for our values of k, c, k_c and c_c, to a first approxi-

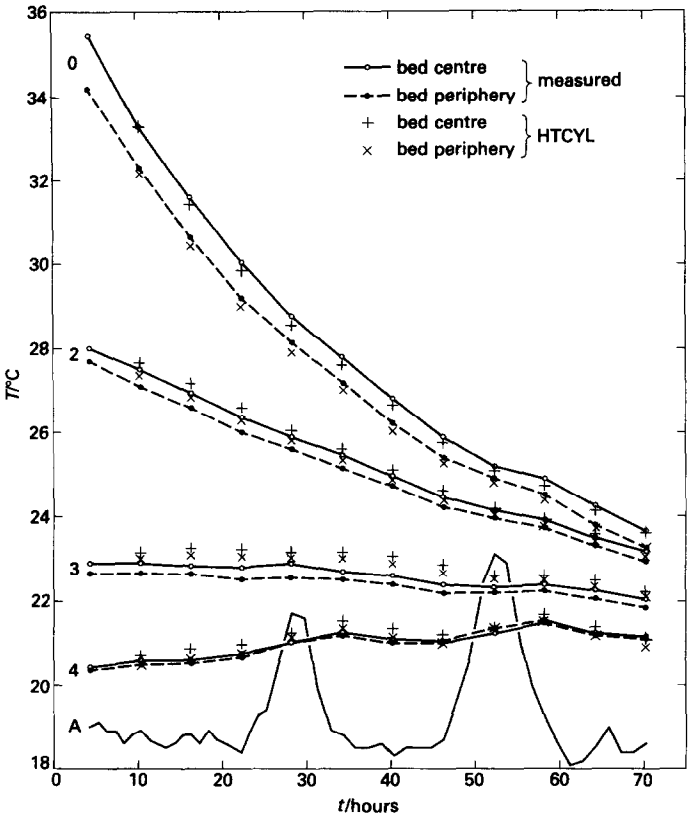

FIG. 3. Temperature variations during a destratification and cooling run on the bed in Fig. 1: experimental values plus values from HTCYL. 0, 2, 3, 4, indicate bed levels, and A ambient. Input values to HTCYL of k, c, k_c and c_c are: $k = 0.55$ W m^{-1} K^{-1}; $c = 1.21 \times 10^6$ J m^{-3} K^{-1}; $k_c = 0.029$ W m^{-1} K^{-1}; $c_c = 4.76 \times 10^4$ J m^{-3} K^{-1}.

mation, the overall cooling rate is given by c/k_c and the destratification rate by c/k.

The level of agreement in Fig. 3 could be improved slightly by adjustments in k, c, k_c and c_c of a few percent. However, given the possibility of inhomogeneities in the bed, and uncertainties in the location of the PRTs at levels 1–4 with respect to those at level 0, it is not clear that any such (small) adjustments are significant.

It is apparent from Fig. 3 that there is a large overall cooling. Overall cooling would have been less prominent had we *either* had a much larger bed, *or* the facility to cool the bed initially below ambient (cf. our measurement method for c_p). Nevertheless, destratification is readily discernible in that the temperature differences between the various levels are less than they would have been in the absence of destratification: k in HTCYL is constrained by the experimental data to a range not exceeding $\pm 10\%$ of the value used. The constraint on c and k_c is somewhat tighter, because of the large overall cooling.

We have thus demonstrated a *general* result, that values of k, c, k_c and c_c from *separate* measurements can be used (with HTCYL or the like) to predict the cooling and destratification of a pebble bed. Moreover, there is no reason to doubt that these are the parameters that control cooling and destratification during charging and recovery also.

The specific results on our particular bed are also of some interest, because a pebble bed with air as the fluid is a type fairly widely used. A practical pebble bed would, in most cases, be larger than ours, and this would make overall cooling less dominant. But in all cases the destratification rate is given, to a *first* approximation, by c/k, where c and k can be measured separately and independently, as outlined in Section 2.2. For our pebble bed, at about 30°C

$$\frac{c}{k} = 610 \pm 30 \text{ h} \tag{13}$$

where the uncertainty in c/k is calculated from those in ρ, c_p and k in Table 1, plus the uncertainty in the (small) temperature adjustment for c. The temperature coefficient of c/k over the approximate range 0–100°C is -0.5 h °C^{-1}, with a large uncertainty of about $\pm 30\%$.

Destratification in beds with $c/k \sim 600$ h will *always* be negligible in those frequent applications where charging and recovery alternate on a time scale of the

order of 24 h or less. When the duty cycle period considerably exceeds the order of 100 h then destratification *can* be significant, in the sense that the temperature of the heat recovered can be considerably lowered because of destratification.

In general, the effect of destratification on recovery temperatures will increase as the duty cycle increases, and as the initial temperature differences along the bed increase. Conversely, the effect of destratification decreases as heat losses increase, because the hotter parts of the bed will cool increasingly more to the surroundings than will the cooler parts, thus leading to greater temperature uniformity regardless of destratification.

Individual cases can be worked out in detail by means of models such as HYCYL and PKBED.

4. CONCLUSIONS

The packed bed investigated here (and specified in some detail in Section 3) has the following properties (see Nomenclature).

(1) The pressure drop Δp across the bed is such that:

(i) $\Delta p \propto l$;

(ii) $\Delta p = a\dot{m} + b\dot{m}^2$;

(iii) the value of Δp is consistent with a previously published correlation [13] (see equation (12) of our work), but not with another previously published correlation [4];

(iv) variations with bed temperature are consistent with the correlations in refs. [4, 13].

(2) The volumetric heat transfer coefficient h_{fs} derived from bed charging is consistent with a previously published correlation [11]

$$h_{fs} = 650\left(\frac{\dot{m}}{A}\frac{1}{d_s}\right)^{0.7}$$

with a (small) correction for the finite diffusivity of individual pebbles.

(3) Values of bed thermal conductivity k and thermal capacity c from separate measurements of each, coupled with the manufacturer's values of k_c and c_c for the container, provide the basis for an adequate description of destratification and cooling of the packed bed.

(4) The type of packed bed that we have investigated (a pebble bed with air as the fluid) exhibits slow destratification such that when charging, or recovery, or any interval between charging and recovery, considerably exceeds the order of 100 h, then destratification can significantly lower recovery temperatures.

Acknowledgements—One of us (MG) is grateful to the Open University for a maintenance grant.

REFERENCES

1. F. W. Schmidt and A. J. Willmott, *Thermal Energy Storage and Regeneration*. McGraw-Hill/Hemisphere, New York (1981).
2. C. Dang-vu and J. Martin, Experimentation on a long term rock-bed thermal storage, *First European Community Conference on Solar Heating*, Amsterdam, 30 April–4 May 1984. Reidel, The Netherlands (1984).
3. H. F. Sullivan, K. G. T. Hollands and E. C. Shewen, Thermal destratification in rock beds, *Solar Energy* **33**, 227–229 (1984).
4. K. G. T. Hollands and H. F. Sullivan, Pressure drops across rock bed thermal storage systems, *Solar Energy* **33**, 221–225 (1984).
5. W. J. Batty, P. W. O'Callaghan and S. D. Probert, Assessment of the thermal-probe technique for rapid, accurate measurements of effective thermal conductivities, *Appl. Energy* **16**, 83–113 (1984).
6. B. W. Jones, Thermal conductivity probe: development of method and application to a coarse granular medium, *J. Phys. E. Scient. Instrum.* **21**, 832–839 (1988).
7. J. K. Roberts and A. D. Miller, *Heat and Thermodynamics*. Blackie, London (1960).
8. BS1042, Methods for the measurement of fluid flow in pipes, Part 1, orifice plates, nozzles and venturi tubes, British Standards Institution, London (1964 and 1968).
9. F. S. Acton, *Numerical Methods that Work*. Harper & Row, London (1970).
10. D. E. Beasley and J. A. Clark, Transient response of a packed bed for thermal energy storage, *Int. J. Heat Mass Transfer* **27**, 1659–1669 (1984).
11. E. C. Shewen, H. F. Sullivan, K. G. T. Hollands and A. R. Balakrishnan, A heat storage subsystem for solar energy, Report STOR-6 Waterloo Research Institute, University of Waterloo, Canada (1978).
12. C. P. Jeffreson, Prediction of breakthrough curves in packed beds, *A.I.Ch.E. Jl* **18**, 409–416 (1972).
13. P. Chandra and D. H. Willits, Pressure drop and heat transfer characteristics of air-rock bed thermal storage systems, *Solar Energy* **27**, 547–553 (1981).

DESTRATIFICATION ET AUTRES PROPRIETES D'UN RESERVOIR CALORIFIQUE FORME D'UN LIT FIXE

Résumé—Un lit fixe se composant de cailloux fluviales est preciscé dans quelque detail. En présente des dounees experimentales sur: la conductibilité calorique et la capacité calorique du lit; la déstratification et le refroidissement du lit. Ces dounées sont mutuellement cohérentes et s'accordent bien avec quelques trauvoux anterieurs et avec nos modèles numeriques du lit.

DESTRATIFICATION UND ANDERE EIGENSCHAFTEN GEPACKTER HITZEBEHALTER

Zusammenfassung—Ein mit Kieselsteinen eng gefülltes Bett ist analytisch beschrieben unterstützt mit experimentellen Daten durch: (a) thermale Konduktivität und Hitzekapazität; (b) die Druckänderung im gefüllten Bett; (c) den volumetrischen Hitzewechsel-Koeffizient zwischen Luftbewegung und den Kieselsteinen und (d) der De-stratification und Kühlung im Bett. Die experimentellen Daten sind in guter Ubereinstimmung mit veröfflentlichten Arbeiten und mit unserem eigenen numerischen Model.

ДЕСТРАТИФИКАЦИЯ И ДРУГИЕ СВОЙСТВА ТЕПЛА, АККУМУЛИРОВАННОГО ПЛОТНЫМ СЛОЕМ

Аннотация—Провадено экспериментальное исследование плотного слоя, состоящего из речной гальки. Приведены экспериментальные данные по теплопроводности и теплоемкости слоя, перепаду давления в слое, объемному коэффициенту теплообмена между потоком воздуха и галькой, дестратификации и охлаждению слоя. Данные хорошо согласуются между собой и с результатами ранее опубликованной работы, а также с разработанными авторами численными моделями слоя.